Proton Conductivity Control by Ion Substitution in a Highly Proton-Conductive Metal−Organic Framework

Masaaki Sadakiyo,*,[†,‡] Teppei Yamada,[†,‖] and Hiroshi Kitagawa*,[†,§]

[†]Division of Chemistry, Graduate School of Science, Kyoto University, Kitashirakawa-Oiwakecho, Sakyo-ku, Kyoto 606-8502, Japan

[‡]International Institute for Carbon-Neutral Energy Research (WPI-I2CNER), Kyushu University, 744 Moto-oka, Nishi-ku Fukuoka 819-0395, Japan

[§]Core Research for Evolutional Science and Technology (CREST), Japan Science and Technology Agency (JST), 7 Goban-cho Chiyoda-ku, Tokyo 102-0076, Japan

Ⓢ *Supporting Information*

ABSTRACT: Proton conductivity through two-dimensional (2-D) hydrogen-bonding networks within a layered metal−organic framework (MOF) $(NH_4)_2(H_2adp)[Zn_2(ox)_3]\cdot3H_2O$ (H_2adp = adipic acid; ox = oxalate) has been successfully controlled by cation substitution. We synthesized a cation-substituted MOF, $K_2(H_2adp)[Zn_2(ox)_3]\cdot3H_2O$, where the ammonium ions in a well-defined hydrogen-bonding network are substituted with non-hydrogen-bonding potassium ions, without any apparent change in the crystal structure. We successfully controlled the proton conductivity by cleavage of the hydrogen bonds in a proton-conducting pathway, showing that the 2-D hydrogen-bonding networks in the MOF truly contribute to the high proton conductivity. This is the first example of the control of proton conductivity by ion substitution in a well-defined hydrogen-bonding network within a MOF.

The control of proton conductivity is important in chemistry, biology, and materials science due to a fundamental interest in understanding proton transport phenomena,[1] as well as potential applications in devices such as gas sensors[2] and fuel cells.[3] Recently, proton conductivity control using metal−organic frameworks (MOFs)[4] is a topic of interest because the ability to rationally design and chemically tune their architecture allows chemists to establish various methods to control the proton conductivity.[5] The well-defined crystalline frameworks of MOFs can allow us to observe the exact structures of the proton-conducting pathways, giving deeper insight into their proton conducting properties.

We have proposed three types (types I−III) of concepts to give high proton conductivity to MOFs.[5a] In type I, proton carriers are introduced as counterions into the pores (e.g., H_3O^+). In type II, acidic groups are placed on the framework (e.g., −COOH). In type III, charge-neutral proton-conducting species are incorporated within the pores (e.g., H_3PO_4). However, for the control of proton conductivity, only types II and III have been realized in actual cases to date.[5c−g] For example, acid functionalization of the terephthalate ligand within MIL-53 has been used to control the proton conductivity in this MOF (type II).[5c] In other examples, amphoteric charge carriers (e.g., imidazole or H_3PO_4) were

introduced into the pores of insulating MOFs to impart various proton-conductive properties to the frameworks (type III).[5f,g] To demonstrate the proton conductivity control of a MOF using the type I concept, there is a requirement that cations playing a critical role for proton transfer within the highly proton-conducting MOF should be possible to be substituted. Furthermore, it is ideal that the structure of proton-conducting pathway does not change due to the ion substitution because the structural change of conducting-pathway might be a major factor for a change of proton conductivity.

In this communication, the focus is on the control of proton conductivity within well-defined proton-conducting pathways by utilizing the type I concept. We were the first to succeed in controlling the proton conductivity by cation substitution (type I) using an analogous proton-conducting pathway without significant change in the main framework. We employed a layered MOF $(NH_4)_2(H_2adp)[Zn_2(ox)_3]\cdot3H_2O$ (H_2adp = adipic acid; ox = oxalate), having both type I and type III features; $(NH_4)_2(H_2adp)[Zn_2(ox)_3]\cdot3H_2O$ shows high proton conductivity because of the existence of two-dimensional (2-D) hydrogen-bonding networks, which act as a crystalline proton-conducting pathway.[5a] We now propose a new way to control proton conductivity through such hydrogen bonded networks utilizing the type I feature of the MOF, namely, changing hydrogen-bonding networks by cation substitution using non-hydrogen-bonding species without changing the crystal structure of the main framework. We report on the effects of ion substitution in a highly proton-conductive MOF to control proton conductivity. We succeeded in constructing a novel MOF, $K_2(H_2adp)[Zn_2(ox)_3]\cdot3H_2O$ (abbreviated as **1·3H₂O**), isostructural with the highly proton-conductive $(NH_4)_2(H_2adp)[Zn_2(ox)_3]\cdot3H_2O$ (**2·3H₂O**),[5a] which has a well-defined proton-conducting pathway. We observed differences in proton conductivity between the potassium-ion-substituted **1·3H₂O** and ammonium-ion-including **2·3H₂O**. Proton conductivity was successfully controlled and the ion-substituted MOF had a conductivity of 1.2×10^{-4} S cm^{-1} under 98% RH at 25 °C, which is 2 orders of magnitude lower than that of the ammonium-ion including **2·3H₂O**, proving the fact that the 2-D hydrogen-bonding networks truly contribute

to the high proton conductivity. We also succeeded in determining the crystal structure of anhydrate phase (**1**), having the same structure as ammonium one (**2**). Herein we describe the synthesis, characterization, and the effect of cation substitution on the proton conductivity in this MOF.

Crystals of **1·3H$_2$O** were synthesized by a hydrothermal method. A mixture of zinc oxide, adipic acid, oxalic acid dihydrate (H$_2$(ox)·2H$_2$O), potassium oxalate monohydrate (K$_2$(ox)·H$_2$O), and water was heated at 130 °C for 24 h (details are shown in the Supporting Information). The crystal structure of **1·3H$_2$O** was determined by single-crystal X-ray diffraction (SCXRD) measurement at 113 K (Figure 1), and

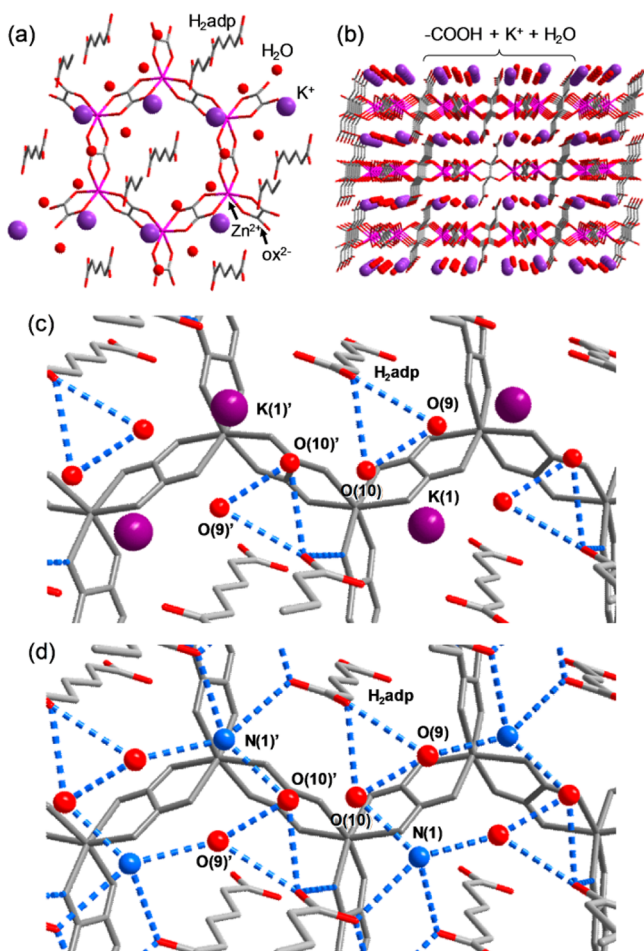**Figure 1.** Crystal structure of **1·3H$_2$O**. Representation of (a) honeycomb-shaped layered structure and (b) 2-D layered structure. Comparison of hydrogen-bonding networks of (c) **1·3H$_2$O** and (d) **2·3H$_2$O**[5a] in the interlayer space.

the parameters of the analysis are shown in Tables S1 and S2, Supporting Information. The anionic component of [Zn$_2$(ox)$_3$]$_\infty^{2-}$, where the zinc ions are octahedrally coordinated by ox ions, forms a typical honeycomb-shaped layered framework that incorporates H$_2$adp molecules vertically. The potassium ions, water molecules, and carboxylic acid groups are located in the interlayer space. As shown in Figure S1, Supporting Information, the positions of the components of the framework and the included guests are almost the same as in the case of the **2·3H$_2$O** except for the existence of potassium ions instead of ammonium ions. It is clear that the replacement of ammonium ions by non-hydrogen-bonding potassium ions

was successfully achieved in this well-defined hydrogen-bonding network, while the structure of the main framework was maintained. Note that the occupancy of the O(10) atom is 50%, as is the case with **2·3H$_2$O**,[5a] indicating that a hydrogen bond is not formed between O(10) and O(10)′, even though the O(10)···O(10)′ distance (2.481(6) Å) is short enough to be recognized as a hydrogen bond.[6] In **1·3H$_2$O**, there are several hydrogen bonds between ox ion and H$_2$adp (O(1)··· O(7), 2.678(2) Å); between H$_2$adp and water molecules (O(7)···O(10), 3.043(4) Å, O(7)···O(9), 3.122(3) Å); and between water molecules (O(9)···O(10); 2.711(7) Å). These distances are close to those of **2·3H$_2$O** (2.688(4), 2.993(8), 3.037(5), and 2.638(12) Å, respectively), confirming that the replacement of ammonium ions by potassium ions does not cause remarkable changes in the arrangement of the guest molecules.

The hydrogen-bonding networks among water, H$_2$adp molecules, and counterions in the 2-D spaces in **1·3H$_2$O** and **2·3H$_2$O** are illustrated in Figure 1c,d. There is a significant difference in the hydrogen-bonding networks between **1·3H$_2$O** and **2·3H$_2$O** due to the existence of non-hydrogen-bonding potassium ions instead of hydrogen-bonding ammonium ions, although the positions of these atoms are almost the same. The several hydrogen bonds associated with the ammonium cations disappeared, as shown in Figure 1c. However, the distances between potassium ions and neighboring atoms in **1·3H$_2$O** are similar to those in **2·3H$_2$O**, while those are not hydrogen bonds, for example, K(1)···O(9) (2.788(4) Å) and N(1)···O(9) (2.850(7) Å); K(1)···O(10) (2.635(3) Å) and N(1)···O(10) (2.789(7) Å); K(1)···O(8) (2.908(2) and 2.742(1) Å) and N(1)···O(8) (2.953(6) and 2.845(4) Å), respectively. This suggests that there should be Coulomb interaction between the positively charged potassium ions and water molecules instead of hydrogen bond formation. Considering that there are significant changes in the 2-D hydrogen-bonding networks in the interlayer space while the main framework structure is maintained, the proton conductivity is expected to differ because this 2-D hydrogen-bonding network likely acts as the proton-conducting pathway, as we previously reported.[5b]

We also performed thermogravimetric analysis and water vapor adsorption measurements to characterize the hydrated phases of the compound. Compound **1·3H$_2$O** showed 8.1% weight loss below 130 °C (Figure S2, Supporting Information), which is attributable to desorption of 3.0 water molecules included in the interlayer space, suggesting that this compound has stoichiometric phases of trihydrate and anhydrate (**1**). It is also clear that the framework structure is stable below 250 °C. Water vapor adsorption analysis was performed using a sample of **1** dried under vacuum at 80 °C overnight. As shown in Figure 2, **1** exhibited a large amount of water vapor adsorption in the low-pressure region, compared with **2·3H$_2$O**, where a two-step water uptake was observed (Figure 2). The amount of adsorption is almost three water molecules at maximum humidity, confirming that there are stoichiometric phases of **1** and **1·3H$_2$O**. Compared with the case of **2·3H$_2$O**, it seems here that the absence of ammonium ions in **1** contributes to a stabilization of the trihydrate phase.

To obtain information about the structure of dehydrated **1**, we performed X-ray powder diffraction (XRPD) measurements (Figure 3). A sample of **1** was sealed in a glass tube after heating at 80 °C under vacuum overnight in order to avoid water exposure. Both **1** and **1·3H$_2$O** had sharp peaks in XRPD patterns, confirming that both are crystalline phases; however,

13167

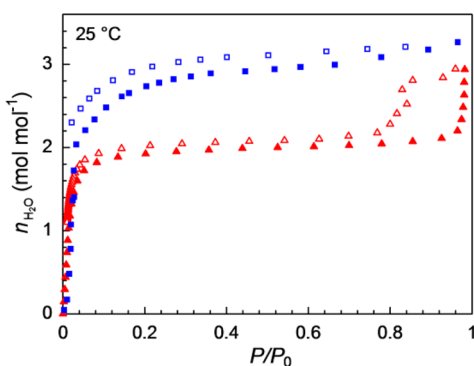dx.doi.org/10.1021/ja507634v | J. Am. Chem. Soc. 2014, 136, 13166−13169

Figure 2. Water vapor adsorption/desorption isotherms of **1** (blue square) and **2** (red triangle)[5b] at 25 °C. Filled and open symbols correspond to adsorption and desorption, respectively.
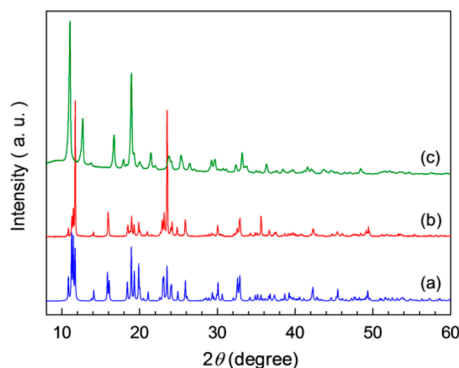

Figure 3. XRPD patterns of (a) **1·3H$_2$O** (simulation from SCXRD data), (b) air-dried sample of **1·3H$_2$O**, and (c) **1**, prepared by heating **1·3H$_2$O** under vacuum at 80 °C overnight.

the pattern of the air-dried sample of **1·3H$_2$O** was completely different to that of **1**, indicating that a structural transformation occurred upon dehydration. To clarify the crystal structure of **1**, we performed Rietveld analysis using the structural model of the anhydrate phase of **2**.[5b] We recognized that the crystal structure of potassium-ion-including **1** is fundamentally the same as that of ammonium-ion-including **2** (Figures S3 and S4 and Table S3, Supporting Information).

To clarify the proton conductivity of the cation-substituted system, we performed ac impedance measurements using a quasi-four-probe method on a pelletized sample (Figures 4 and
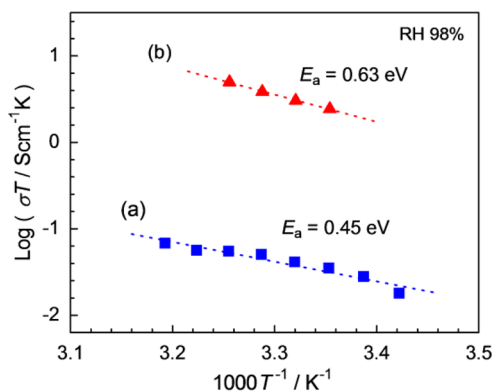

Figure 4. Arrhenius plots of the proton conductivity of (a) **1·3H$_2$O** under 98% RH (blue). A reported value of (b) **2·3H$_2$O** is also shown for comparison (red).[5a] Least-squares fitting is shown as a dotted line.

S5, Supporting Information). The hydrated **1·3H$_2$O** showed proton conductivity of 1.2×10^{-4} S cm^{-1} at 25 °C under maximum humidity conditions of 98% RH, which is approximately 2 orders of magnitude lower than that of **2·3H$_2$O** (0.8×10^{-2} S cm^{-1}, 25 °C, 98% RH)[5a] under the same conditions. Considering that the guest arrangement and framework structure of **1·3H$_2$O** is almost the same as that of **2·3H$_2$O**, the decrease in proton conductivity of **1·3H$_2$O** must arise from the difference in the counter cations; the hydrogen-bonding networks in **2·3H$_2$O** truly contribute to its high proton conductivity, and the ammonium ions play a critical role in promoting high proton conductivity within the well-defined hydrogen-bonding networks. Ammonium ions should play two roles in the proton conduction in this system; the first is to increase proton carrier in the pores due to their acid character (pK_a = 9.2), and the second is to promote proton transport by formation of a hydrogen-bonding network with neighboring atoms. The relatively high proton conductivity of **1·3H$_2$O** (1.2×10^{-4} S cm^{-1}, 25 °C) suggests that there should exist another proton-conducting pathway consisting of adipic acid and water molecules, even though the conductivity is lower than **2·3H$_2$O**. We think that 1-D channels consisting of O(10) and O(9) (Figure 1c) contribute to the proton-conducting pathway even though there is a relatively long distance between O(9) and O(9)′ (3.442(3) Å, slightly long for a hydrogen bond), which is similar to **2·3H$_2$O**.[5b] The results of further studies on neutron scattering measurements for **1·3H$_2$O** and **2·3H$_2$O** revealed that rotational motion of ammonium ions also plays an important role in the higher proton conductivity in **2·3H$_2$O**, as is reported previously.[7] It should be noted that this is the first example of the successful control of proton conductivity using the type I feature (cation substitution) in the well-defined hydrogen-bonding networks of a MOF. From the Arrhenius plots, measured under 98% RH (Figure 4), the activation energy (E_a) of proton conductivity in **1·3H$_2$O** was estimated to be 0.45 eV. The value of E_a is still relatively high[8] compared with that of typical hydrated proton conductors, which conduct through a Grotthuss mechanism,[9] such as Nafion.[10] As mentioned in the previous paper,[5a] we are of the opinion that such a high value of E_a in this closely packed proton-conducting pathway, where the Grotthuss mechanism is likely occur, is partially derived from some other process, such as the direct diffusion of additional protons with water molecules (the vehicle mechanism[11]), as estimated from the half-occupied oxygen sites of O(10) in **1·3H$_2$O**. We also measured the proton conductivity of the anhydrate **1** under helium atmosphere (0% RH) after dehydration under vacuum. The conductivity of **1** at room temperature was determined to be 2.2×10^{-12} S cm^{-1}, which has almost the same value as that of **2** (1.4×10^{-12} S cm^{-1}).[5b] This clearly indicates that the counter cations do not migrate in the interlayer space even with some space around them and that the conductivity of the hydrated state **1·3H$_2$O** is purely due to the proton transport. The conducting mechanism of the hydrated phase is likely a Grotthuss-type mechanism, and the ion substitution significantly affects the proton conductivity.

In conclusion, we have demonstrated the first example of proton conductivity control in a MOF using the type I concept. We have succeeded in synthesizing a novel MOF including potassium counter cations instead of ammonium ions in a 2-D layered framework making it isomorphous to the highly proton-conductive ammonium phase. By cation substitution within the well-defined proton-conducting pathway, the conductivity is significantly altered, while the 2-D layered framework structure

is maintained. The potassium-ion-substituted MOF exhibited proton conductivity that was two orders lower than that of an ammonium-ion-including MOF with the same crystal structure. This result is an important demonstration of proton conductivity control using MOFs and may offer a general method to impart or enhance the proton-conducting properties to MOFs through ion substitution.

■ ASSOCIATED CONTENT

Ⓢ Supporting Information

Synthesis, physical measurements, and X-ray analysis data; X-ray crystallographic file in CIF format. This material is available free of charge via the Internet at http://pubs.acs.org.

■ AUTHOR INFORMATION

Corresponding Authors

sadakiyo@i2cner.kyushu-u.ac.jp.
kitagawa@kuchem.kyoto-u.ac.jp.

Present Address

∥Center for Molecular Systems (CMS), Department of Chemistry and Biochemistry, Graduate School of Engineering, Kyushu University, Moto-oka 744, Nishi-ku, Fukuoka, 819-0395, Japan.

Notes

The authors declare no competing financial interest.

■ ACKNOWLEDGMENTS

■ REFERENCES

(1) (a) Royant, A.; Edman, K.; Ursby, T.; Pebay-P, E.; Landau, E. M.; Neutze, R. Nature 2000, 406, 645−648. (b) Voth, G. A. Acc. Chem. Res. 2006, 39, 143−150.

(2) Yamazoe, N.; Shimizu, Y. Sens. Actuators 1986, 10, 379−398.

(3) (a) Haile, S. M.; Boysen, D. A.; Chisholm, C. R. I.; Merle, R. B. Nature 2001, 410, 910−913. (b) Kreuer, K. D.; Paddison, S. J.; Spohr, E.; Schuster, M. Chem. Rev. 2004, 104, 4637−4678.

(4) (a) Gándara, F.; Furukawa, H.; Lee, S.; Yaghi, O. M. J. Am. Chem. Soc. 2014, 136, 5271−5274. (b) Kitagawa, S.; Kitaura, R.; Noro, S. Angew. Chem., Int. Ed. 2004, 43, 2334−2375. (c) Murray, L. J.; Dinca, M.; Long, J. R. Chem. Soc. Rev. 2009, 38, 1294−1314. (d) Li, J. R.; Sculley, J.; Zhou, H. C. Chem. Rev. 2011, 112, 869−932. (e) Lee, J. Y.; Farha, O. K.; Roberts, J.; Scheidt, K. A.; Nguyen, S. T.; Hupp, J. T. Chem. Soc. Rev. 2009, 38, 1450−1459. (f) Rocca, J. D.; Liu, D.; Lin, W. Acc. Chem. Res. 2011, 44, 957−968. (g) Kurmoo, M. Chem. Soc. Rev. 2009, 38, 1353−1379. (h) Sadakiyo, M.; Kasai, H.; Kato, K.; Takata, M.; Yamauchi, M. J. Am. Chem. Soc. 2014, 136, 1702−1705. (i) Takaishi, S.; Hosoda, M.; Kajiwara, T.; Miyasaka, H.; Yamashita, M.; Nakanishi, Y.; Kitagawa, Y.; Yamaguchi, K.; Kobayashi, A.; Kitagawa, H. Inorg. Chem. 2009, 48, 9048−9050. (j) Kitagawa, H. Nat. Chem. 2009, 1, 689−690. (k) Yamada, T.; Otsubo, K.; Makiura, R.; Kitagawa, H. Chem. Soc. Rev. 2013, 42, 6655−6669.

(5) (a) Sadakiyo, M.; Yamada, T.; Kitagawa, H. J. Am. Chem. Soc. 2009, 131, 9906−9907. (b) Sadakiyo, M.; Yamada, T.; Kitagawa, H. J. Am. Chem. Soc. 2014, 136, 7701−7707. (c) Shigematsu, A.; Yamada, T.; Kitagawa, H. J. Am. Chem. Soc. 2011, 133, 2034−2036. (d) Jeong, N. C.; Samanta, B.; Lee, C. Y.; Farha, O. K.; Hupp, J. T. J. Am. Chem. Soc. 2012, 134, 51−54. (e) Kim, S.; Dawson, K. W.; Gelfand, B. S.; Taylor, J. M.; Shimizu, G. K. H. J. Am. Chem. Soc. 2013, 135, 936−966. (f) Bureekaew, S.; Horike, S.; Higuchi, M.; Mizuno, M.; Kawamura, T.; Tanaka, D.; Yanai, N.; Kitagawa, S. Nat. Mater. 2009, 8, 831−836. (g) Ponomareva, V. G.; Kovalenko, K. A.; Chupakhin, A. P.; Dybtsev, D. N.; Shutova, E. S.; Fedin, V. P. J. Am. Chem. Soc. 2012, 134, 15640−

15643. (h) Ōkawa, H.; Shigematsu, A.; Sadakiyo, M.; Miyagawa, T.; Yoneda, K.; Ohba, M.; Kitagawa, H. J. Am. Chem. Soc. 2009, 131, 13516−13522. (i) Ōkawa, H.; Sadakiyo, M.; Yamada, T.; Maesato, M.; Ohba, M.; Kitagawa, H. J. Am. Chem. Soc. 2013, 135, 2256−2262. (j) Sadakiyo, M.; Ōkawa, H.; Shigematsu, A.; Ohba, M.; Yamada, T.; Kitagawa, H. J. Am. Chem. Soc. 2012, 134, 5472−5475. (k) Kitagawa, H.; Nagao, Y.; Fujishima, M.; Ikeda, R.; Kanda, S. Inorg. Chem. Commun. 2003, 6, 346−348. (l) Taylor, J. M.; Mah, R. K.; Moudrakovski, I. L.; Ratcliffe, C. I.; Vaidhyanathan, R.; Shimizu, G. K. H. J. Am. Chem. Soc. 2010, 132, 14055−14057. (m) Umeyama, D.; Horike, S.; Inukai, M.; Kitagawa, S. J. Am. Chem. Soc. 2013, 135, 11345−11350. (n) Pardo, E.; Train, C.; Gontard, G.; Boubekeur, K.; Fabelo, O.; Liu, H.; Dkhil, B.; Lloret, F.; Nakagawa, K.; Tokoro, H.; Ohkoshi, S.; Verdaguer, M. J. Am. Chem. Soc. 2011, 133, 15328−15331.

(6) Kuleshova, L. N.; Zorkii, P. M. Acta Crystallogr. 1981, B37, 1363−1366.

(7) Miyatsu, S.; Kofu, M.; Nagoe, A.; Yamada, T.; Sadakiyo, M.; Yamada, T.; Kitagawa, H.; Tyagi, M.; Sakai, V. G.; Yamamuro, O. Phys. Chem. Chem. Phys. 2014, 16, 17295−17304.

(8) (a) Baffier, N.; Badot, J. C.; Colomban, P. Solid State Ionics 1980, 2, 107−113. (b) Perrino, C. T.; Wentrcek, P. J. Solid State Chem. 1974, 10, 36−38. (c) Casciola, M.; Costantino, U. Solid State Ionics 1986, 20, 69−73. (d) Badot, J. C.; Colomban, Ph. Solid State Ionics 1989, 35, 143−149. (e) Howe, A. T.; Shilton, M. G. J. Solid State Chem. 1980, 34, 149−155.

(9) Agmon, N. Chem. Phys. Lett. 1995, 244, 456−462.

(10) Sone, Y.; Ekdunge, P.; Simonsson, D. J. Electrochem. Soc. 1996, 143, 1254−1259.

(11) Kreuer, K. D.; Rabenau, A.; Weppner, W. Angew. Chem., Int. Ed. 1982, 21, 208−209.